Publication Year	2016
Acceptance in OA	2020-05-12T08:23:35Z
Title	Seasonal exposure of carbon dioxide ice on the nucleus of comet 67P/Churyumov-Gerasimenko
Authors	FILACCHIONE, GIANRICO, RAPONI, Andrea, CAPACCIONI, FABRIZIO, CIARNIELLO, Mauro, TOSI, Federico, Capria, M. T., DE SANCTIS, MARIA CRISTINA, MIGLIORINI, Alessandra, PICCIONI, GIUSEPPE, Cerroni, P., Barucci, M. A., Fornasier, S., Schmitt, B., Quirico, E., Erard, S., Bockelee-Morvan, D., Leyrat, C., Arnold, G., MENNELLA, Vito, Ammannito, E., BELLUCCI, Giancarlo, Benkhoff, J., Bibring, J. P., Blanco, A., Blecka, M. I., Carlson, R., Carsenty, U., COLANGELI, Luigi, Combes, M., Combi, M., Crovisier, J., Drossart, P., Encrenaz, T., Federico, C., Fink, U., Fonti, S., Fulchignoni, M., Ip, W. -H., Irwin, P., Jaumann, R., Kuehrt, E., Langevin, Y., Magni, G., McCord, T., Moroz, L., Mottola, S., PALOMBA, Ernesto, Schade, U., Stephan, K., Taylor, F., Tiphene, D., Tozzi, G. P., Beck, P., Biver, N., Bonal, L., Combe, J. -Ph., Despan, D., Flamini, E., FORMISANO, Michelangelo, FRIGERI, ALESSANDRO, GRASSI, Davide, Gudipati, M. S., Kappel, D., Longobardo, A., Mancarella, F., Markus, K., Merlin, F., OROSEI, ROBERTO, RINALDI, GIOVANNA, CARTACCI, MARCO, Cicchetti, A., Hello, Y., Henry, F., Jacquinod, S., Reess, J. M., NOSCHESE, RAFFAELLA, POLITI, ROMOLO, Peter, G.
Publisher's version (DOI)	10.1126/science.aag3161
Handle	http://hdl.handle.net/20.500.12386/24717
Journal	SCIENCE
Volume	354

Title: Seasonal exposure of carbon dioxide ice on the nucleus of comet 67P/Churyumov-Gerasimenko

Authors: G. Filacchione[1*], A. Raponi[1], F. Capaccioni[1], M. Ciarniello[1], F. Tosi[1], M. T. Capria[1], M. C. De Sanctis[1], A. Migliorini[1], G. Piccioni[1], P. Cerroni[1], M. A. Barucci[2], S. Fornasier[2], B. Schmitt[3], E. Quirico[3], S. Erard[2], D. Bockelee-Morvan[2], C. Leyrat[2], G. Arnold[4], V. Mennella[5], E. Ammannito[6], G. Bellucci[1], J. Benkhoff[7], J. P. Bibring[8], A. Blanco[9], M. I. Blecka[10], R. Carlson[11], U. Carsenty[3], L. Colangeli[7], M. Combes[2], M. Combi[12], J. Crovisier[2], P. Drossart[2], T. Encrenaz[2], C. Federico[13], U. Fink[14], S. Fonti[9], M. Fulchignoni[2], W. H. Ip[15], P. Irwin[16], R. Jaumann[3], E. Kuehrt[3], Y. Langevin[8], G. Magni[1], T. McCord[17], L. Moroz[4], S. Mottola[4], E. Palomba[1], U. Schade[18], K. Stephan[4], F. Taylor[16], D. Tiphene[2], G. P. Tozzi[19], P. Beck[3], N. Biver[2], L. Bonal[3], J-Ph. Combe[17], D. Despan[2], E. Flamini[20], M. Formisano[1], A. Frigeri[1], D. Grassi[1], M. S. Gudipati[11], D. Kappel[4], A. Longobardo[1], F. Mancarella[9], K. Markus[4], F. Merlin[2], R. Orosei[21], G. Rinaldi[1], M. Cartacci[1], A. Cicchetti[1], Y. Hello[2], F. Henry[2], S. Jacquinod[2], J. M. Reess[2], R. Noschese[1], R. Politi[1], G. Peter[22]

Affiliations:

[1]INAF-IAPS, Istituto Nazionale di AstroFisica - Istituto di Astrofisica e Planetologia Spaziali, Rome, Italy.

[2]LESIA, Laboratoire d'Études Spatiales et d'Instrumentation en Astrophysique, Observatoire de Paris, PSL Research University, CNRS - Centre National de la Recherche Scientifique, Sorbonne Universités, UPMC Univ. Paris 06, Univ. Paris Diderot, Sorbonne Paris Cité, France

[3]Univ. Grenoble Alpes, CNRS - Centre National de la Recherche Scientifique, IPAG, Grenoble, France.

[4]Institute for Planetary Research, DLR - Deutschen Zentrums für Luft- und Raumfahrt, Berlin, Germany.

[5]INAF Istituto Nazionale di AstroFisica - Osservatorio di Capodimonte, Neaples, Italy.

[6]UCLA - University of California, Los Angeles, USA.

[7]ESA European Space Agency – ESTEC - European Space Research and Technology Centre, Noordwjik, The Netherlands.

[8]Institut d'Astrophysique Spatial CNRS - Centre National de la Recherche Scientifique, Orsay, France.

[9]Dipartimento di Matematica e Fisica "Ennio De Giorgi", Università del Salento, Lecce, Italy.

[10]Space Research Centre, Polish Academy of Sciences, Warsaw, Poland.

[11]NASA JPL – Jet Propulsion Laboratory, Pasadena, USA.

[12]Space Physics Research Laboratory, The University of Michigan, Ann Arbor, USA.

[13]Università di Perugia, Perugia, Italy.

[14]Lunar Planetary Laboratory, University of Arizona, Tucson, USA.

[15]National Central University, Taipei, Taiwan.

[16]Departement of Physics, Oxford University, Oxford, UK.

[17]Bear Fight Institute, Winthrop, WA, USA.

[18]Helmholtz-Zentrum Berlin für Materialien und Energie, Berlin, Germany.

[19]INAF Istituto Nazionale di AstroFisica - Osservatorio Astrofisico di Arcetri, Firenze, Italy.

[20]Agenzia Spaziale Italiana, Rome, Italy.

[21]INAF Istituto Nazionale di AstroFisica - Istituto di Radioastronomia, Bologna, Italy.

[22]Institute of Optical Sensor Systems, DLR - Deutschen Zentrums für Luft- und Raumfahrt, Berlin, Germany.

*Correspondence to: gianrico.filacchione@iaps.inaf.it, phone +39-0645488454

Abstract:

Carbon dioxide is one of the most abundant species in cometary nuclei, but due to its high volatility CO_2 ice is generally only found beneath the surface. We report the infrared spectroscopic identification of a CO_2 ice-rich surface area, located in the Anhur region of comet 67P/Churyumov-Gerasimenko. Spectral modeling shows that about 0.1% of the 80×60 m area is CO_2 ice. This exposed ice was observed a short time after exiting from local winter; following the increased illumination, the CO_2 ice completely disappeared over about three weeks. We estimate the mass of the sublimated CO_2 ice and the depth of the surface eroded layer. The presence of CO_2 ice is interpreted as the result of the extreme seasonal changes induced by the rotation and orbit of the comet.

One Sentence Summary: Quantitative characterization of CO_2 ice sublimating on the surface of 67P/CG's nucleus due to seasonal effect.

Main Text:

On comets, sublimation due to solar illumination is the major mechanism creating the differentiation of volatile species over their long dynamical lifetimes. The penetration of the heat into the nucleus causes chemical stratification with more volatile molecules, such as CO and CO_2, receding into the interior ices, while less volatile molecules, such as water, remain close to the surface and enrich the near surface ices ***(1)***. The seasonal variability associated with the relatively large orbital eccentricities of comets is further complicated by the irregular shape of the nuclei and by the inclination of their rotation axis, which amplifies the seasonal effects. Thermal evolution models so far did not provide evidence of recondensation neither of fast sublimation of volatile species following an extreme seasonal cycle. 67P/Churyumov-Gerasimenko (67P/CG) confirmed the general volatiles stratification scheme, during the pre-perihelion period, when the spatial distribution of water vapor and carbon dioxide in the gaseous coma was interpreted as due to CO_2 ice sublimating from inner layers, with H_2O ice sublimating closer to the surface ***(2,3,4,5,6)***. On the other hand, a diurnal cycle of water ice has been found where an ephemeral frost layer is formed following sudden shadowing conditions and day/night variation ***(7)***.

In early 2015 the southern hemisphere of 67P/CG was emerging from shadows and leaving its cold season, when sub-surface temperatures were maintained as low as 25-50 K ***(8)***. In particular, an area located in the Anhur region (at lon=66.06°, lat= -54.56° in Cheops coordinate frame ***(9)***), experienced a four-year-long winter season before being illuminated by the Sun in mid-January 2015.

We used the VIRTIS-M (Visible, InfraRed and Thermal Imaging Spectrometer, Mapping Channel) onboard the Rosetta spacecraft ***(10)*** to detected a carbon dioxide ice-rich area in Anhur region on March 21-22 2015 when the comet was at 2.05 AU from the Sun. This region is 80 by

60 m (resolved at 20 m/pixel on VIRTIS-M images), shown in the general context of the nucleus' digital shape model in ***Fig. 1***. The deposit is located in a smooth area of the Anhur region, placed on the large lobe of the nucleus ***(11)***. The same spectral dataset, for which we give additional details in ***(12)***, has been used to derive quantitative information on CO_2 abundance. The irradiance/solar flux (I/F) spectrum of the pixel showing the more intense absorption features is shown in ***Fig. 2.*** The I/F is characterized by a steep red spectral slope shortward of 1.5 μm, an absorption triplet at 1.97, 2.01, 2.07 μm, and two further absorptions at 2.7 and 2.78 μm. These features correspond to known absorption features of CO_2 so identify the presence of CO_2 ice on the surface of 67P/CG. The CO_2 ice fundamental band at 4.26 μm is not visible on I/F spectra due to the thermal emission from the nucleus. A detailed description of the spectral variability across the CO_2 ice rich area, the removal of thermal emission and spectral modeling are given in ***(12***).

The spectra of the CO_2 ice rich area have been fitted with a radiative transfer model ***(13,14)*** allowing us to derive quantitative information on endmember abundances, mixing modalities and grain sizes. The I/F spectrum is simulated by using areal and intimate mixtures of two components: the Dark Terrain (DT) unit, corresponding to the measured average organic-rich spectrum of the comet's surface ***(15)*** after the application of photometric correction ***(16)*** and carbon dioxide ice derived from optical constants ***(17,18)***. The composition of the Dark Terrain unit, characterized by low albedo, red slope and a broad absorption feature in the 3.2 μm range, is still uncertain ***(19).*** In order to check the quality of the spectral retrieval, an additional fit has been performed by replacing carbon dioxide ice with crystalline water ice ***(20,21,22)***. The VIRTIS spectral mixing and data processing methods are described at length in previous works ***(23,24)***. The modeling of each individual pixel on which CO_2 ice is detected is discussed in ***(12*)*.***

The results of the spectral modeling are shown in the left panel of ***Fig. 2.*** The best fitting model including a water ice component requires 99.7% DT with a slope (necessary to correct for photometric response) of -3.8% μm^{-1} plus 32 μm water ice grains in areal mixing for the remaining 0.3%. The quality of this fit is very poor however (χ^2=3.85), in particular in the 2.0 μm and 2.7-2.8 μm ranges where water ice is not able to reproduce the observed absorption features, indicating its absence in this area. Better fits are achieved by replacing H_2O with CO_2 ice, as also shown in ***Fig. 2.*** We show two possible models. The first corresponds to an intimate mixing ***(12)*** of 99.2% DT with a -5.12% μm^{-1} slope plus 0.8% of CO_2 ice grains of 800 μm size. The second case corresponds to an areal mixing of 99.9% DT with a slope of -4.76% μm^{-1} plus 0.1% of 50 μm size CO_2 ice grains. With a residual of χ^2=2.05, the areal solution appears marginally better than the intimate which has χ^2=2.45. The addition of water ice to the components of the mixture does not improve the fit quality. In both models less than 1% of CO_2 ice is sufficient to account for the observed spectral absorption features.

The CO_2 ice features have been detected on two consecutive days (21 and 22 March 2015). This means that the CO_2 ice area was stable against day-night variations in the temperature. However, after the March detection, VIRTIS-M did not observe the Anhur area again until April 12-13 2015, when the heliocentric distance was reduced to 1.87 AU and the pixel scale is reduced from 20 to 39 m/pixel. At this time the spectra acquired did not show any of the previously observed CO_2 absorption features (***Fig. 3***), indicating that the CO_2 ice patch had retreated to a level below the detection limit of the VIRTIS-M instrument (band depth less than 1% relative to the local continuum, corresponding to <0.1% CO_2 ice abundance), if not disappeared altogether. The reduction of the spatial resolution by a factor about 2 and the increase of the solar phase angle from 54° to 79° occurring between the two sets of observations

must be considered in interpreting the disappearance of the CO_2 ice spectral features: apart the change in spatial resolution, the last images are more affected by long shadows caused by local topography, making the detection of the CO_2 ice more difficult. Conversely, assuming a uniform distribution of CO_2 ice in areal mixing with the DT within the initial 80 by 60 m area, one should expect to detect it also on the less resolved images because the instrumental resolution is still within the size of the area of interest.

The maximum surface temperature *T*, derived by modeling the 4.5-5.0 μm thermal emission using a Bayesian method ***(25)***, in this area increased from *T*=218.8 K on 21 March 2015 to *T*=225.9 K on 13 April 2015. However, as the surface is not isothermal at the sub-pixel scale due to local roughness and shadows, these should be considered as an upper limit, representative only of the warmest fractions of the pixel, corresponding to the more illuminated sub-pixel areas. The measured temperatures are well above the sublimation temperature of CO_2 ice, which is about 80 K ***(26)***, therefore the CO_2 ice-rich region cannot be in thermal equilibrium with the DT and continuous sublimation must occur. For this reason the intimate mixing between CO_2 ice and DT is much less favorable than the areal. As a result of the sublimation of the volatile species on the surface an increase of the local roughness on the more illuminated areas is very likely to occur.

The illumination history of the Anhur CO_2 ice-rich area has been investigated by tracing the variation of the incident solar flux during the time when VIRTIS-M observations were available. Throughout the period January 2011 - January 2015 the Anhur region was in permanent shadow while from January 14 2015 the combined effect of decreasing heliocentric distance and longer insolation caused a net increase of solar flux on the area (***Fig. 4***). After scaling the instantaneous solar flux with the cosine of the incidence angle calculated using the nucleus digital shape model ***(27,28)***, we found that at the time of the carbon dioxide ice detection (March 21-22 2015) the maximum solar flux at local noon was about 80 W/m^2 (***Fig. 4***). At the time of the second series of VIRTIS-M observations the maximum solar flux at local noon had increased to about 135 W/m^2.

The integrated solar flux accumulated by an area of 0.4 m^2, corresponding to the CO_2 areal occupancy within the 400 m^2 VIRTIS-M pixel, is equal to 2.026×10^7 J over 45 rotations of the comet occurring between the VIRTIS-M available observations. Assuming a CO_2 ice latent heat of sublimation of 552 kJ/kg ***(26)*** and neglecting the thermal conduction in view of the very low thermal inertia reported for 67P/CG (***8,29***), we derive (further details are given in ***(12)***) a value for the total amount of sublimated ice of 35 kg, equivalent to the erosion of a 5.6 cm thick layer. This value is an upper limit, assuming a complete sublimation of the ice during 45 rotations. A similar estimate, performed from the beginning of the illumination conditions in early January 2015 until the time of the carbon dioxide ice detection, gives an additional sublimated ice mass of 22 kg. Hence, the area within a VIRTIS-M pixel has experienced a maximum sublimation of 57 kg of CO_2 ice, corresponding to an erosion of a 9 cm layer, in about three months. The temporal trend of the cumulative CO_2 ice sublimation mass is shown in ***Fig. 4***.

This amount of sublimated CO_2 ice is too small to contribute significantly to the gaseous coma emissions. Above the south hemisphere VIRTIS has detected a CO_2/H_2O ratio of about 4% ***(4)*** but no evidence has been found of increased H_2O or CO_2 gaseous activity in the surrounding of the Anhur region from VIRTIS-M spectra. In fact, even assuming a sublimation rate of 1 kg of CO_2 ice per day from a 20 by 20 m area, the resulting column density of 10^{17} m^{-2} in the ambient coma is about two orders of magnitude lower than the average value of 10^{19} m^{-2} measured by VIRTIS-M ***(4)***.

The observation of the CO_2 ice-rich spot was unexpected at these heliocentric distances due to the high volatility of carbon dioxide; water ice, a less volatile species, was not observed in the same region at the same time, as sustained by spectral fit shown in ***Fig. S5*** in ref. (***12***). 67P/CG falls in the ensemble of the CO_2 rich comets as demonstrated by the high activity level of CO_2 above the southern hemisphere where the ratio CO_2/H_2O is considerably larger than in the northern hemisphere (***4,30***).

The OSIRIS instrument did observe water ice in this same region (***31***) in April-May 2015, about six weeks after the initial detection of the CO_2 ice by VIRTIS-M. At this time, by 4 May 2015, the VIRTIS-M IR channel has stopped operating, due to the permanent failure of the active cooler, making impossible to further study the temporal evolution of the Anhur area. Until then, the entire part of the southern hemisphere illuminated by the Sun was observed by VIRTIS-M with a spatial resolution between 20 and 40 m/pixel. So far, the presence of the CO_2 ice has been recognized only in the Anhur area discussed in this study, localized approximately between a slope and a flat terrain showing a regular topography on OSIRIS images ***(31)***. The morphology and the illumination conditions above this place are similar to many other neighborhood areas observed by VIRTIS-M.

The presence of CO_2 ice at the surface of the nucleus thus appears to be an ephemeral occurrence, which provides clues to the emplacement mechanism. After perihelion passage, the activity of a cometary nucleus starts to decrease, with water sublimation decreasing first. Nucleus thermodynamical modeling (***1***) shows that a stratigraphy associated to the volatility of the major gaseous species is produced on the outer layers. However, the combination of spin axis inclination and nucleus shape is such that the Anhur CO_2 ice-rich area experiences a fast drop in the illumination going into permanent shadow quickly after equinox and, consequently, quickly reducing the surface temperatures in winter to less than T=80 K, while the interior remains warmer for a longer time due to the low thermal inertia ***(8,29)***. Sublimation of water ice at depth is prevented but not that of CO_2, which can continue to flow from the interior to the surface where it begins to freeze due to the low surface temperatures. Moving further towards the aphelion, the low surface temperatures are able to preserve the CO_2 ice on the surface and to grow >100 μm size grains until, on the next orbit, it is exposed again to sunlight and sublimates away. This inverse-temperature profile of cometary surfaces (warmer inside and cooler on the surface) going into winter (in permanently shadowed regions) subsequent to perihelion could potentially freeze other volatiles that are sublimed from the warmer interior as well. Based on the temperature of these surface areas, more volatiles species such as CO and CH_4 could also be frozen until the next exposure to solar photons occurs. The same phenomenon could also explain why no water ice was seen at this site during the initial exposure to the sun, as the H_2O-ice would have been frozen at lower depths than the CO_2 ice.

In summary, the 67P/CG nucleus shows two different temporal activity cycles caused by H_2O and CO_2 ices present in different regions: while water ice has diurnal variability, with surface sublimation and condensation cycle occurring in the most active areas ***(7)***, the surface condensation of carbon dioxide ice has a seasonal dependence. Similar processes are probably common among many Jupiter family comets, which share with 67P/CG short revolution periods and eccentric orbits ***(32)***.

References and Notes:

(1) De Sanctis, M. C., Capria, M. T., Coradini, A., 67P/Churyumov–Gerasimenko nucleus model: Portrait of the Rosetta target. *Advances in Space Research*, **38**, 1906-1910 (2006).

(2) Hässig, M. et al. Time variability and heterogeneity in the coma of 67P/Churyumov-Gerasimenko. *Science*, **347** (2015).

(3) Bockelée-Morvan, et al. First observations of H_2O and CO_2 vapor in comet 67P/Churyumov-Gerasimenko made by VIRTIS onboard Rosetta. *Astron. Astrophys.*, **583**, id.A6, 14 pp (2015).

(4) Migliorini, A. et al. Water and carbon dioxide distribution in the 67P/Churyumov-Gerasimenko coma from VIRTIS-M infrared observations. *Astron. Astrophys.*, **589**, id A45, 12 pp. (2016).

(5) Fougere, N. et al., Three-dimensional direct simulation Monte-Carlo modeling of the coma of comet 67P/Churyumov-Gerasimenko observed by the VIRTIS and ROSINA instruments on board the Rosetta. *Astron. Astrophys.*, **588**, id A124, 11 pp. (2016).

(6) Fink, U. et al, Investigation into the disparate origin of CO_2 and H_2O outgassing for Comet 67/P. *Icarus*, **277**, 19 pp. (2016).

(7) De Sanctis, M. C. et al. The diurnal cycle of water ice on comet 67P/Churyumov-Gerasimenko. *Nature*, **525**, 500-503 (2015).

(8) Choukroun, M. et al., Dark side of comet 67P/Churyumov-Gerasimenko in Aug.-Oct. 2014. MIRO/Rosetta continuum observations of polar night in the southern regions. *Astron. Astrophys.,* **583**, A28 (2015).

(9) Preusker, F. et al., Shape model, reference system definition, and cartographic mapping standards for comet 67P/Churyumov-Gerasimenko - Stereo-photogrammetric analysis of Rosetta/OSIRIS image data. *Astron. Astrophys.,* **583**, A33 (2015)**.**

(10) Coradini, A. et al. VIRTIS: an imaging spectrometer for the Rosetta mission. *Space Sci. Rev.,* **128**, 529-559 (2007).

(11) El-Maarry, M. R. et al., Regional surface morphology of comet 67P/Churyumov-Gerasimenko from Rosetta/OSIRIS images: The southern hemisphere. *Astron. Astrophys*., **593**, A110 (2016).

(12) Materials and methods are available as supplementary materials on Science Online.

(13) Hapke, B. *Theory of Reflectance and Emittance Spectroscopy*, Cambridge Univ. Press (2012).

(14) Ciarniello, M. et al., Hapke modeling of Rhea surface properties through Cassini-VIMS

spectra. *Icarus* **214**, 541-555 (2011).

(15) Capaccioni, F., et al., The organic-rich surface of comet 67P/Churyumov-Gerasimenko as seen by VIRTIS/Rosetta. *Science* **347**, (2015).

(16) Ciarniello, M. et al. Photometric properties of comet 67P/Churyumov-Gerasimenko from VIRTIS-M onboard Rosetta. *Astron. Astrophys.* **583**, A31 (2015).

(17) Quirico, E. & Schmitt, B. Near-Infrared Spectroscopy of Simple Hydrocarbons and Carbon Oxides Diluted in Solid N_2 and as Pure Ices: Implications for Triton and Pluto. *Icarus* **127**, 354-378 (1997).

(18) Quirico, E., et al., Composition, physical state and distribution of ices at the surface of Triton, *Icarus* **139**, 159-178, (1999).

(19) Quirico, E. et al., Refractory and semi-volatile organics at the surface of comet 67P/Churyumov-Gerasimenko: Insights from the VIRTIS/Rosetta imaging spectrometer, *Icarus* **272**, 32-47 (2016).

(20) Warren, S. G. Optical constants of ice from the ultraviolet to the microwave. *Appl. Opt.* **23**, 1206 (1984).

(21) Mastrapa, R. M. et al. Optical constants of amorphous and crystalline H2O-ice: 2.5-22 μm (4000-455 cm–1) optical constants of H_2O-ice. *Astrophys. J.* **701**, 1347-1356 (2009).

(22) Clark, R. N. et al. The surface composition of Iapetus: mapping results from Cassini VIMS. *Icarus* **218**, 831-860 (2012).

(23) Filacchione G., et al. Exposed water ice on the nucleus of comet 67P/Churyumov-Gerasimenko. *Nature* **529** (2016a).

(24) Filacchione, G., et al. The global surface composition of 67P/CG nucleus by Rosetta/VIRTIS. I) Prelanding mission phase. *Icarus* **274**, 334-349 (2016b).

(25) Tosi, F. et al. Thermal measurements of dark and bright surface features on Vesta as derived from Dawn/VIR. *Icarus* **240**, 36-57 (2014).

(26) Huebner, W. F et al., *Heat and Gas Diffusion in Comet Nuclei*, ISSI report SR-004, June, 2006. ISBN 1608-280X. Published for The International Space Science Institute, Bern, Switzerland, by ESA Publications Division, Noordwijk, The Netherlands, (2006).

(27) Jorda, L., & Gaskell, R. H. *Shape models of 67P/Churyumov-Gerasimenko*, RO-C-OSINAC/OSIWAC-5-67P-SHAPE-V1.0, NASA Planetary Data System and ESA Planetary Science Archive (2015), available from https://pds.jpl.nasa.gov/ds-view/pds/viewDataset.jsp?dsid=RO-C-OSINAC%2FOSIWAC-5-67P-SHAPE-V1.0

(28) Jorda, L. et al., The Global Shape, Density and Rotation of Comet 67P/Churyumov-Gerasimenko from Pre–Perihelion Rosetta/OSIRIS Observations. *Icarus* **277**, 257-278 (2016).

(29) Schloerb, F.P., et al., MIRO observations of subsurface temperatures of the nucleus of 67P/Churyumov-Gerasimenko. *Astron. Astrophys.* **583**, A29, pp. 11 (2015).

(30) Bockelée-Morvan, D. et al., Pre/Post perihelion asymmetry of H_2O, CO_2, CH_4 and OCS outgassing in comet 67P from Rosetta/VIRTIS-H observations. *MNRAS*, in press, http://dx.doi.org/10.1093/mnras/stw2428.

(31) Fornasier, S. et al., Rosetta's comet 67P sheds its dusty mantle to reveal its icy nature, *Science*, under review.

(32) Jewitt, D. Cometary rotation: an overview. *Earth, Moon and Planets* **79**, 35-53, (1997).

(33) Ammannito, E. et al. On-ground characterization of Rosetta/VIRTIS-M. I. Spectral and geometrical calibrations. *Rev. Sci. Instrum*. **77**, 093109 (2006).

(34) Filacchione, G. et al. On-ground characterization of Rosetta/VIRTIS-M. II. Spatial and radiometric calibrations. *Rev. Sci. Instrum*. **77**, 103106 (2006).

(35) Filacchione, G. Calibrazioni a terra e prestazioni in volo di spettrometri ad immagine nel visibile e nel vicino infrarosso per l'esplorazione planetaria. *PhD dissertation, Univ. Studi di Napoli Federico II* (2006); available at: http://www.fedoa.unina.it/1462/1/Filacchione_Ingegneria_Aerospaziale_Navale_e_della_Qualita.pdf.

(36) Migliorini, A. et al. Comparative analysis of airglow emissions in terrestrial planets, observed with VIRTIS-M instruments on board Rosetta and Venus Express. *Icarus* **226**, 1115–1127 (2013).

(37) Raponi, A., 2014, Spectrophotometric analysis of cometary nuclei from in situ observations, PhD Thesis, Universià degli studi di Roma Tor Vergata, available at: http://arxiv.org/abs/1503.08172

(38) http://rredc.nrel.gov/solar/spectra/am0/modtran.html

(39) Acton, C. H., Ancillary data services of NASA's Navigation and Ancillary Information Facility, *Planet. Space Sci.* **44**, 65-70 (1996).

(40) Barucci, M.A. et al., Detection of exposed H2O ice on the nucleus of comet 67P/Churyumov-Gerasimenko as observed by Rosetta OSIRIS and VIRTIS instruments. *Astron. Astrophys*. in press, DOI: http://dx.doi.org/10.1051/0004-6361/201628764.

(41) Protopapa, S. et al., Water ice and dust in the innermost coma of comet 103P/Hartley 2, *Icarus* **238**, 191-204 (2014).

Acknowledgments:

The authors would like to thank the following institutions and agencies, which supported this work: Italian Space Agency (ASI - Italy), Centre National d'Etudes Spatiales (CNES- France), Deutsches Zentrum für Luft- und Raumfahrt (DLR-Germany), National Aeronautic and Space Administration (NASA-USA). VIRTIS was built by a consortium from Italy, France and Germany, under the scientific responsibility of IAPS, Istituto di Astrofisica e Planetologia Spaziali of INAF, Rome (IT), which lead also the scientific operations. The VIRTIS instrument development for ESA has been funded and managed by ASI, with contributions from Observatoire de Meudon financed by CNES and from DLR. The VIRTIS instrument industrial prime contractor was former Officine Galileo, now Leonardo SpA in Campi Bisenzio, Florence, IT. The authors wish to thank the Rosetta Liaison Scientists, the Rosetta Science Ground Segment and the Rosetta Mission Operations Centre for their support in planning the VIRTIS observations. The VIRTIS calibrated data are available through ESA's Planetary Science Archive (PSA) web site (http://www.cosmos.esa.int/web/psa/rosetta). This research has made use of NASA's Astrophysics Data System.

Figures captions:

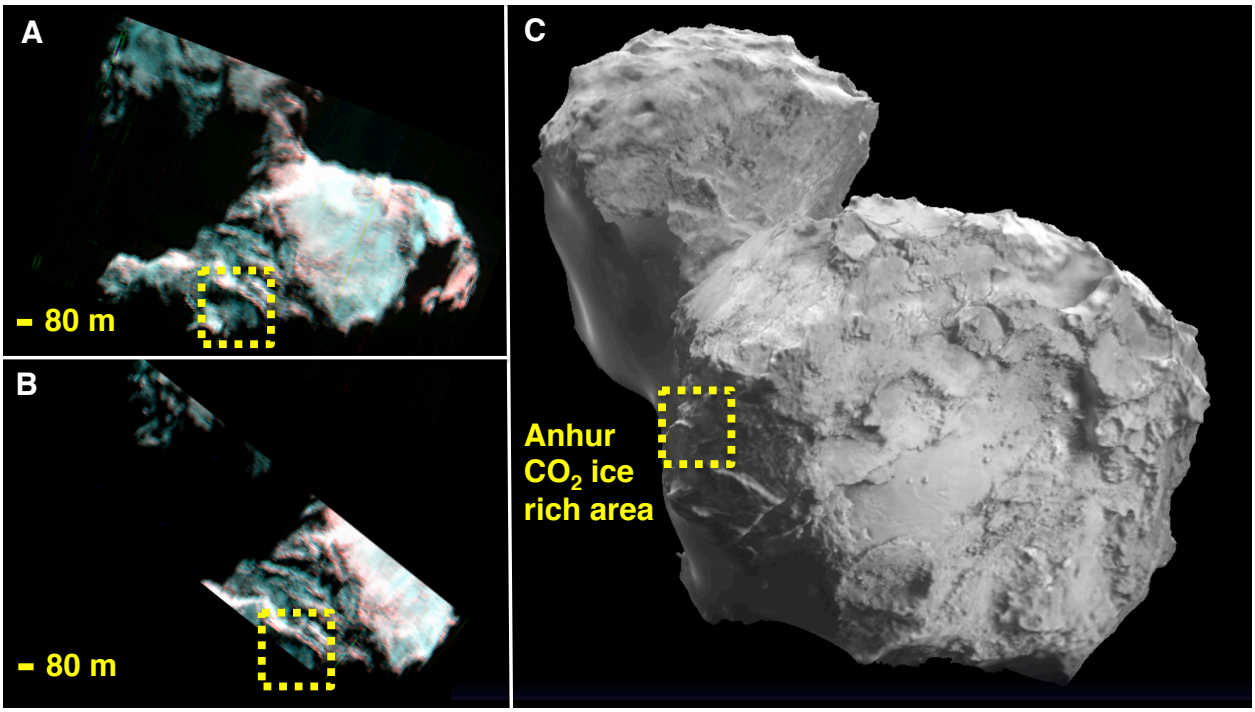

Fig. 1. VIRTIS-M infrared images of the Anhur CO_2 Ice-Rich Area on March 21-22 2015. The center of the yellow line dashed area indicates the location of the carbon dioxide rich patch

on two VIRTIS-M images (I1_00385598211 in panel A and I1_00385688463 in panel B) and on the nucleus shape model rendering (from http://sci.esa.int/comet-viewer/?model=esa, panel C). VIRTIS-M color images are a RGB combination of IR bands (blue at 1.2 μm, green at 2.0 μm and red at 4.0 μm). A description of the VIRTIS-M acquisitions is given in ***(12)*.**

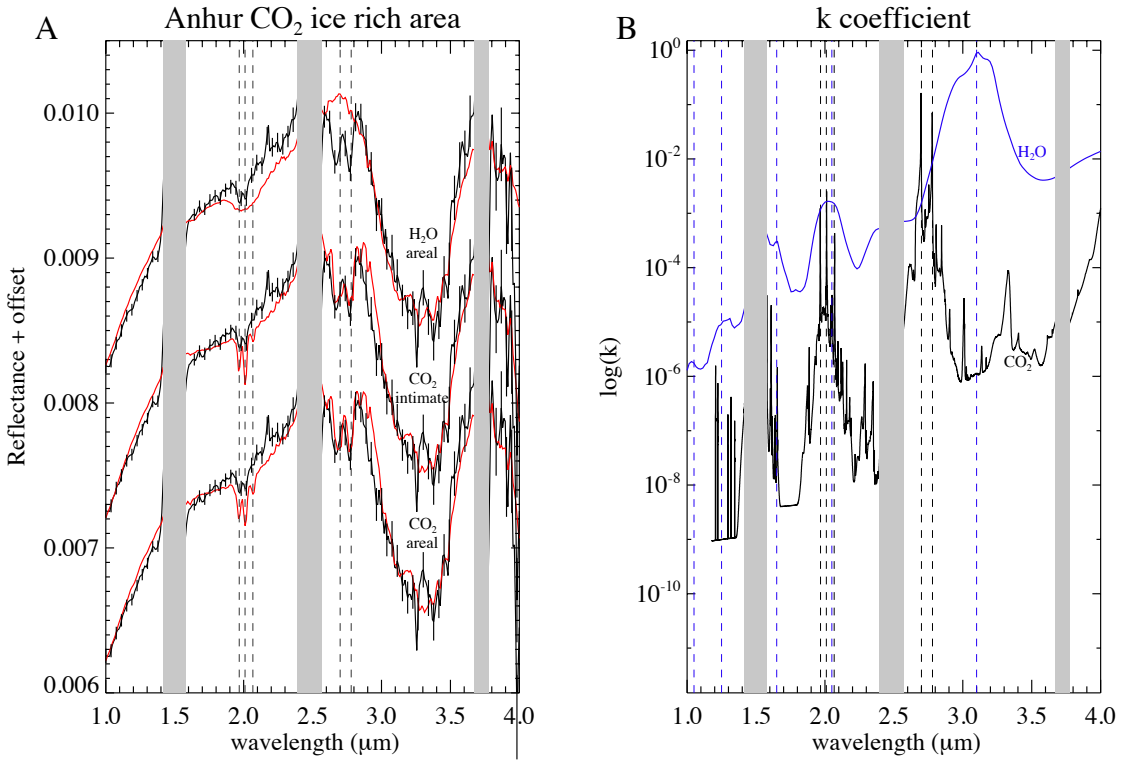

Fig. 2. Spectral modeling of the CO_2 surface ice on March 21 2015 observation. Panel A: VIRTIS-M reflectance (black curve, from observation I1_00385598211, pixel s=126, l=109) and spectral simulations carried out with Dark Terrain (DT) and H_2O ice in areal mixing (top, plus 0.002 offset), DT and CO_2 ice in intimate mixing (centre, plus 0.001 offset) and areal mixing (bottom) for the Anhur CO_2 ice-rich area. Spectral intervals marked in gray correspond to missing data due to instrumental order sorting filters. Error bars, shown every 5 bands to improve readibilty, give the instrument noise on the pixel. A description of VIRTIS-M acquisitions is given in ***(12)*.** Panel B: imaginary part k of refractive indices for H_2O ice (blue curve) and CO_2 ice (black curve). Optical constants for CO_2 are from ref. ***(17,18)*** and for H_2O from ref. ***(20,21,22)***. Vertical lines mark the k local maxima corresponding to the strongest absorption bands at 1.05, 1.25, 1.65, 2.05, 3.10 μm for H_2O (in blue color) and at 1.97, 2.01, 2.07, 2.70, 2.78 μm for CO_2 ice (in black color, also shown in panel A).

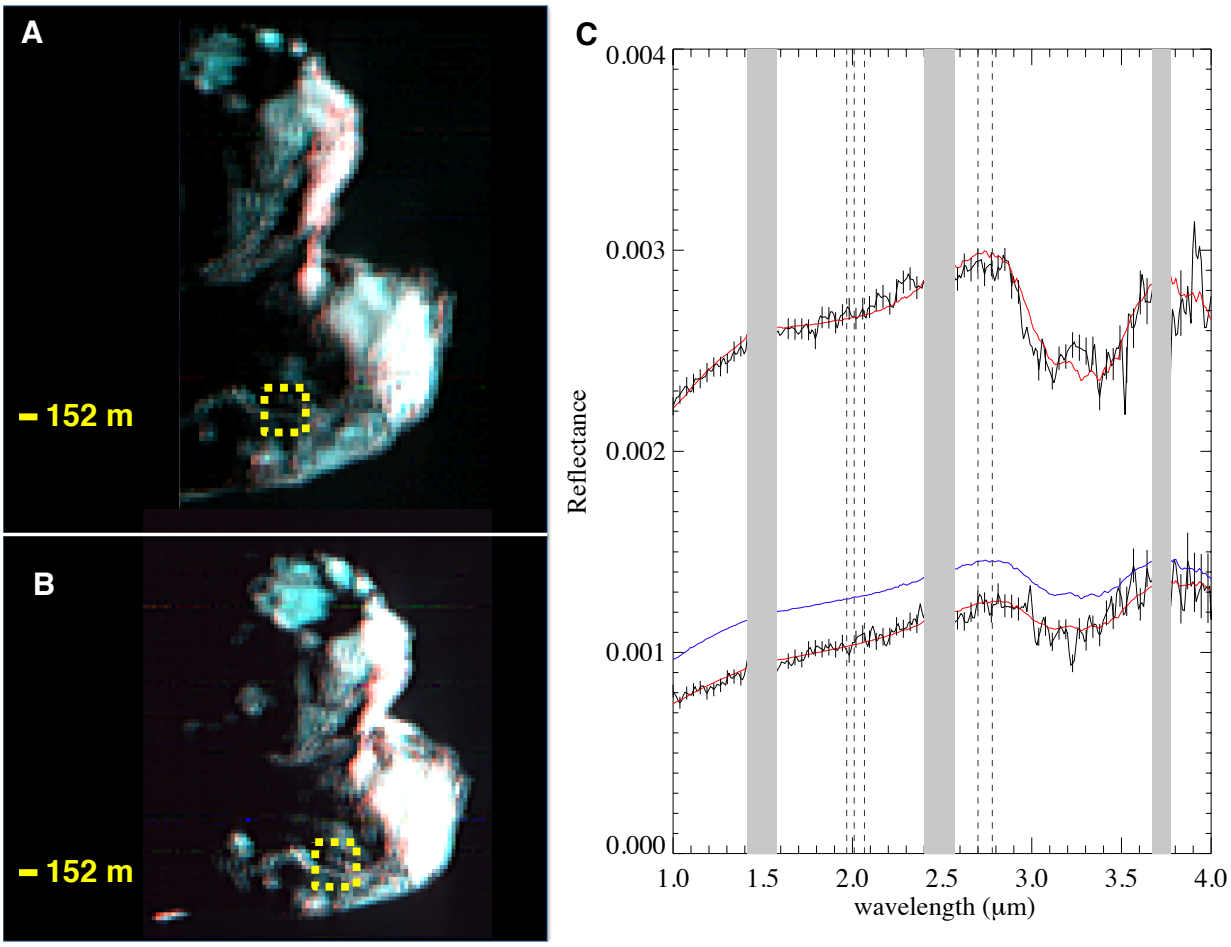

Fig. 3. The disappearance of the CO_2 surface ice by April 12-13 2015: VIRTIS-M acquisitions I1_00387470597 (panel A and bottom black plot on panel C) and I1_00387561494 (panel B and top black plot on panel C). Spectral modeling results with pure Dark Terrain (DT) are shown in red for the two acquisitions. The position of the Anhur CO_2 ice deposit previously observed is marked by the center of the yellow line dashed area. Panel C: reflectance of the Anhur CO_2 ice-rich area on the two acquisitions do not show the diagnostic triplet absorption at 2.0 μm nor the bands at 2.7 and 2.78 μm (dashed vertical lines). The wide feature at 3.2 μm is the DT absorption due to organic material which show a depth correlated with the local reflectance level. For reference, the average DT reflectance as derived from Ref. ***(16)*** is shown (blue curve). A description of VIRTIS-M acquisitions and spectral modeling are given in ***(12)*.**

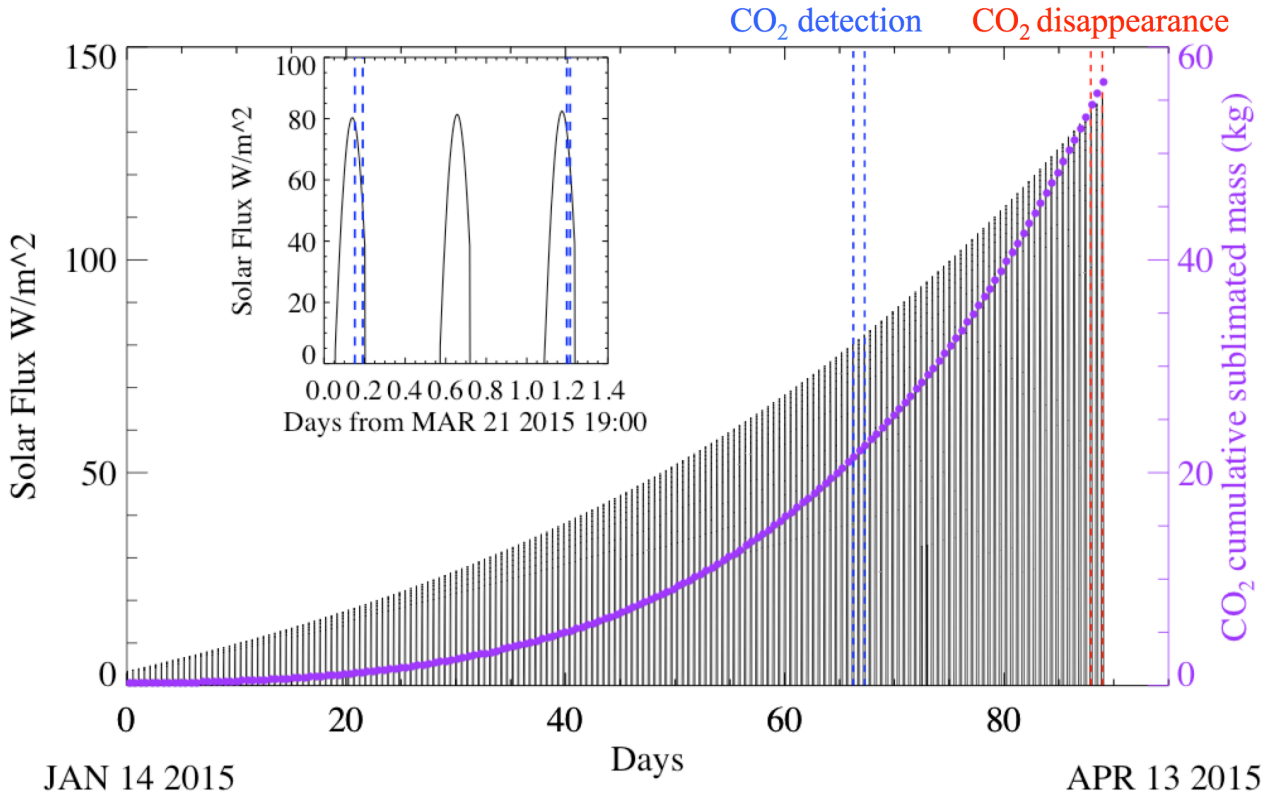

Fig. 4. Variation of the solar flux reaching Anhur CO_2 ice rich area between January 14 - April 13 2015. The vertical dashed lines indicate the time of the four VIRTIS observations described in the text: CO_2 ice has been detected during the first two (marked in blue, see zoom in the inset panel) while it has disappeared in the last two (marked in red). The CO_2 cumulative sublimated mass during this timeframe is shown by the purple curve. All values are relative to one VIRTIS pixel area (20 by 20 m) at the time of the CO_2 detection.